Structure Elucidation

International Edition: DOI: 10.1002/anie.201503657
German Edition: DOI: 10.1002/ange.201503657

Discovery and Structure Determination of an Unusual Sulfide Telluride through an Effective Combination of TEM and Synchrotron Microdiffraction**

*Felix Fahrnbauer, Tobias Rosenthal, Tilo Schmutzler, Gerald Wagner, Gavin B. M. Vaughan, Jonathan P. Wright, and Oliver Oeckler**

Dedicated to Professor Juri Grin on the occasion of his 60th birthday

Abstract: *The structure elucidation of the novel sulfide telluride $Pb_8Sb_8S_{15}Te_5$ demonstrates a new versatile procedure that exploits the synergism of electron microscopy and synchrotron diffraction methods for accurate structure analyses of side-phases in heterogeneous microcrystalline samples. Suitable crystallites of unknown compounds can be identified by transmission electron microscopy and relocated and centered in a microfocused synchrotron beam by means of X-ray fluorescence scans. The refined structure model is then confirmed by simulating HRTEM images of the same crystallite. $Pb_8Sb_8S_{15}Te_5$ consists of chains of heterocubane-like units. Cation coordination polyhedra form unusually entwined chains of edge- and face-sharing bicapped trigonal prisms. The structure data are precise enough for bond-valence calculations, which confirm the disordered atom distribution. On this basis, optimization of physical properties becomes feasible.*

Many solid-state syntheses of metastable materials include rapid quenching processes that often lead to poorly crystalline materials. Intriguing new phases may be present only as side-phases and can hint at reaction mechanisms if they correspond to intermediate phases in a sequence of reactions. Conventional X-ray diffraction is not suitable for the characterization of such microcrystalline multiphase mixtures, especially if unknown structures are present. Whereas laboratory single-crystal X-ray diffraction is limited to crystals larger than approximately 1000 μm^3, microfocused synchrotron radiation allows the collection of data from specimens smaller than 1 μm^3. However, selecting and mounting such microcrystals from multiphase samples is extremely tedious and used to involve numerous attempts until a suitable specimen of a minority phase was accidentally found. On the other hand, new developments in electron crystallography have yielded a plethora of structure analyses from micro- or nanocrystals. However, owing to dynamical diffraction effects and various experimental limitations, structures solved from electron data cannot be refined with enough precision for detailed discussions. Site-occupancy factors or anisotropic displacement parameters, as well as the accuracy of bond lengths, are not comparable to those of standard X-ray crystallography, even when dynamic effects are taken into account to some extent.[1] Furthermore, many techniques are restricted to X-rays, for example, special sample environments and the use of anomalous dispersion to differentiate elements with similar electron counts or to determine the absolute configuration.

For many sulfides and tellurides, large crystals of stable samples for straightforward structure analyses are frequently accessible by chemical vapour transport or occur as minerals. $Pb_2Sb_2S_5$ (plumosite) and $Pb_2Bi_2S_5$ (cosalite), for example, adopt chain-like structures with NaCl-type fragments.[2] The polar bonding results in rather low electrical conductivity. In contrast, the corresponding tellurides exhibit layer-like structures with NaCl-type slabs as building blocks and are significantly better electrical conductors.[3] The combination of the vast structural variety of sulfides with the electrical properties of tellurides makes sulfide tellurides an intriguing class of compounds, with potential applications in thermoelectrics or photovoltaics with a tuneable bandgap, for example. For several decades, research on sulfide tellurides focused on Bi_2Te_2S (tetradymite) and the homologous series $(PbS)_nBi_2Te_2S$.[4] These stable layered compounds are characterized by completely ordered anions. However, homogeneous phases in the system Pb/Sb/Te/S are difficult to access since many reactions tend to afford binary lead chalcogenides in addition to other products.[5] Novel and possibly metastable compounds in this system might, however, be flexible enough to tolerate S and Te at one position despite their different

[*] F. Fahrnbauer, T. Schmutzler, Priv.-Doz. Dr. G. Wagner, Prof. Dr. O. Oeckler
Institute for Mineralogy, Crystallography and Materials Science
Leipzig University, Scharnhorststr. 20, 04275 Leipzig (Germany)
E-mail: oliver.oeckler@gmx.de
Dr. T. Rosenthal
Department of Chemistry, University of Munich (LMU)
Butenandtstr. 5-13, 81377 Munich (Germany)
Dr. G. B. M. Vaughan, Dr. J. P. Wright
ESRF-The European Synchrotron
71, avenue des Martyrs, 38000 Grenoble (France)

[**] Financial support from the European Union (European Social Fund, NFG "Effiziente Energienutzung: Neue Konzepte und Materialien") and the Deutsche Forschungsgemeinschaft (Grant OE530/3-1) is gratefully acknowledged. The authors thank Dr. L. Erra (ESRF, Grenoble) for help during the synchrotron experiments. Furthermore, we are indebted to Prof. Dr. W. Schnick (LMU Munich) for his generous support of this work.

Supporting information for this article (including crystal selection procedure, PXRD data, additional HRTEM and SAED simulations and bond valence calculations) is available on the WWW under http://dx.doi.org/10.1002/anie.201503657.

covalent radii. Partial anion ordering may be a possibility for continuous variation of the electrical properties and could thus make sulfide tellurides more versatile than the "intermediate" selenides.

Attempts to partially substitute S by Te in boulangerite-type $Pb_5Sb_4S_{11}$[6] yielded a mixture of PbTe, Sb_2Te, and an unknown quaternary phase in quenched melts of the nominal starting composition "$Pb_5Sb_4S_6Te_5$".[7] Broadened and overlapping reflections as well as further side-phases as confirmed by SEM (scanning electron microscopy), impede structure analysis from powder X-ray diffraction (PXRD) data. Selected-area electron diffraction (SAED) patterns of the quaternary phase (see the Supporting Information) revealed tetragonal metrics ($a = 7.64$ Å, $c = 15.18$ Å) that correspond neither to unit cells of typical "sulfosalts" nor to lattice parameters known from related classes of compounds. Energy-dispersive X-ray spectroscopy (EDX) of such crystals yielded the composition $Pb_{20.5(3)}Sb_{23.2(7)}S_{42.0(7)}Te_{14(1)}$, which approximately corresponds to that of the novel phase $Pb_8Sb_8S_{15}Te_5$ (see below). Several attempts to optimize the synthesis did not yield single crystals of suitable size for laboratory X-ray diffraction. Annealing the original samples, for example, did not yield a significantly larger fraction of the quaternary phase according to PXRD patterns compared to the quenched sample. Therefore, a finely ground inhomogeneous sample of quenched "$Pb_5Sb_4S_6Te_5$" was dispersed on a carbon-coated transmission electron microscopy (TEM) grid. A well-crystallized part of a quaternary fragment was chosen by means of EDX and SAED. The tip of this crystal (about $0.3 \times 0.5 \times 1\ \mu m^3$ in size) was recovered at beamline ID11 (ESRF, Grenoble) by a telescope with large magnification as well as by X-ray fluorescence, using the copper crossbars of the grid as "landmarks". The crystallite was centered through fluorescence line scans for Cu, Sb, S, and Te (Figure 1). The single-crystal dataset was then collected using a $0.7 \times 2\ \mu m^2$ microfocused synchrotron beam.

The structure of $Pb_8Sb_8S_{15}Te_5$ was solved with direct methods in space group $P4_1$.[8] Twinning around [110] as indicated by the seemingly higher Laue symmetry close to 4/*mmm* and additional inversion twinning were taken into account. Mixed occupancies were refined on all positions; negligible occupancies were set to zero in the final refinement. Detailed information on the refinement strategy and results are given in the Supporting Information. The structure model is confirmed by the excellent match of simulated high-resolution TEM images (defocus series) with experimental ones obtained from the same crystallite as used for synchrotron measurements (Figure 2).

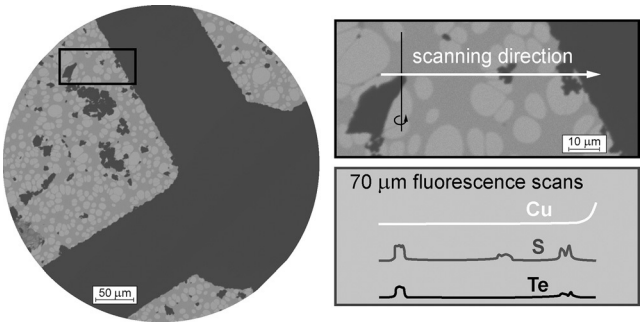

Figure 1. TEM image of the selected crystallite on a copper grid (left) and an enlarged image of the measured tip of the crystallite ($0.3 \times 0.5 \times 1\ \mu m^3$) with center of rotation (top right), and a schematic representation of fluorescence line scans of Cu, Te and S (bottom right). The copper crossbar functions as a "landmark"; a side-phase visible in the center of the scan contains no Te, whereas the crystals on the right side of the scans are located too close to the copper bar to be measured independently.

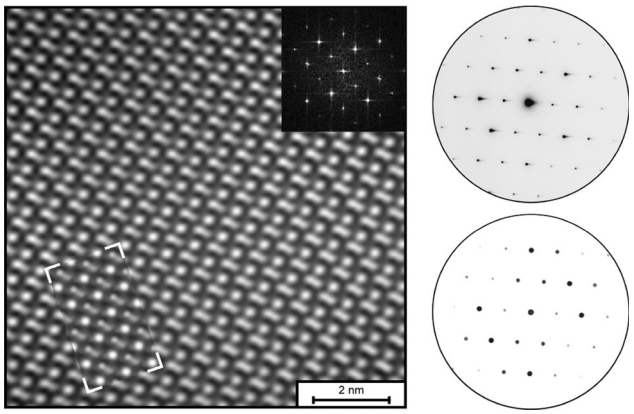

Figure 2. Fourier-filtered HRTEM image (left) of $Pb_8Sb_8S_{15}Te_5$ along zone axis [21$\bar{1}$] with simulation (inset bottom left; multislice method, sample thickness 11.7 nm, defocus −80 nm), Fourier transform (inset, top right), corresponding experimental (top right) and simulated (bottom right) SAED patterns. Further simulations can be found in the Supporting Information.

$Pb_8Sb_8S_{15}Te_5$ is isostructural to Tl_3PbCl_5 and the high-temperature modification of Tl_3PbBr_5 (both $P4_1$).[9] The higher symmetry $P4_12_12$, which was discussed for Tl_3PbCl_5,[10] is clearly absent for $Pb_8Sb_8S_{15}Te_5$. The structure consists of chains of distorted single-side-capped heterocubane-like units along [001], which resemble distorted NaCl-type building blocks. Within the chains, these cubes are interconnected via mixed Pb/Sb positions and S (but not Te) atoms (Figure 3). The cation coordination is similar to the one in comparable sulfides, for example, in boulangerite-type $Pb_5Sb_4S_{11}$. Owing to lone electron pair effects, three S and S/Te neighbors form a trigonal pyramid as the first coordination sphere of Sb and Pb/Sb atoms. Whereas in $Pb_5Sb_4S_{11}$, four anions located farther away complete the coordination polyhedron to a single-capped trigonal prism, these polyhedra are much more distorted in $Pb_8Sb_8S_{15}Te_5$ and better described as bicapped trigonal prisms, taking into account an eighth S/Te neighbor. Four different chains of cation-centered polyhedra correspond to the four cation sites (Figure 4). Chains 1 and 2 are built up of edge-sharing bicapped trigonal prisms with greater amplitudes than chains 3 and 4, which are formed by face-sharing polyhedra. Each of the latter chains is entwined by one edge-sharing chain via common faces, which results in a staggered arrangement of two different "superchains" in the structure. These are interconnected via faces shared by chains 1 and 2 as well as chains 3 and 4.

Site occupancies were confirmed by bond-valence calculations, which match the refinement results very well. Sites

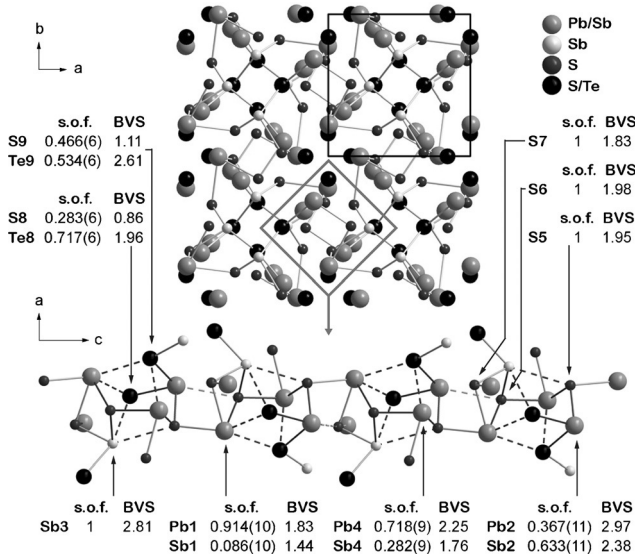

Figure 3. Projection of the structure of $Pb_8Sb_8S_{15}Te_5$ (top, unit cell outlined in the top right part) and side-view of one characteristic chain of heterocubane-like units (bottom). Bonds are indicated and additional connections for completing the building blocks are given as dashed lines (bond valences of these are <0.25 and interatomic distances >3 Å).

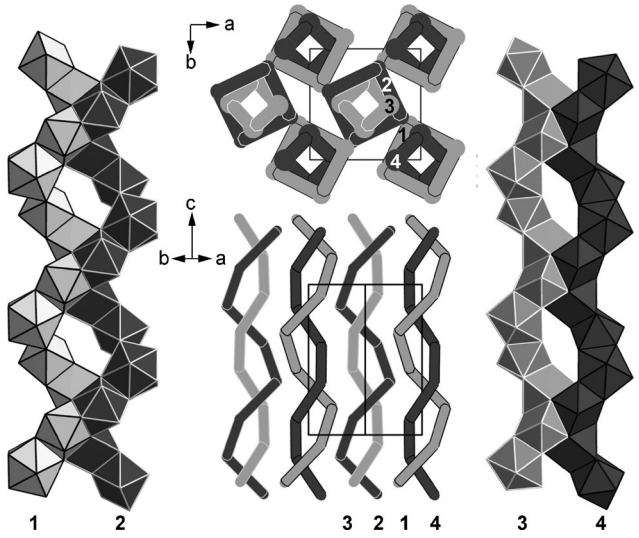

Figure 4. Chains of cation-centered polyhedra in $Pb_8Sb_8S_{15}Te_5$: edge-sharing chains (1 and 2, left) and face-sharing chains (3 and 4, right) of trigonal prisms. Chains 1 and 3 and chains 2 and 4 are entwined to form "superchains" (bottom middle, interchain connection of 1 and 4 as well as 2 and 3 via common faces not shown). The relative arrangement of the "superchains" is shown above (top middle). Anions omitted for clarity.

that are exclusively occupied by one atom type show a deviation of less than 9% from the ideal values. Since the covalent radii of S and Te or Sb and Pb differ, the coordination spheres of mixed sites represent an average. Mixed occupation was taken into account by weighting the bond valences by the occupancy factors, which leads to a deviation from the ideal values, but in turn proves the assumption of mixed occupation. This is also consistent with the anisotropic displacement parameters, which increase with a higher degree of mixed occupation. For example, the mean displacement parameter for Sb2/Pb2 with 40% Pb occupation is 2.3 times larger than that of Sb3, which is fully occupied by Sb.

In contrast to previous unsuccessful attempts based on the approximate composition determined by EDX, phase-pure $Pb_8Sb_8S_{15}Te_5$ could be obtained once the exact composition was known from the structure analysis. However, this is only possible by quenching small amounts of stoichiometric melts and annealing finely ground samples for several days. As an example, the thermoelectric properties of pressed and sintered bulk material were determined. $Pb_8Sb_8S_{15}Te_5$ undergoes a p-type/n-type transition at 200 °C and an n-type/p-type one at 450 °C. In combination with a rather low electrical conductivity, which might be due to the polar bonding character of the predominant sulfur atoms and/or incomplete sintering processes, this limits the thermoelectric Figure of merit ZT to technologically irrelevant values (Figure S8 in the Supporting Information). Based on a detailed knowledge of the structure, optimization of the electrical conductivity can now be efficiently approached. For example, the atom coordination spheres indicate that the Te content may be increased, which would be expected to yield higher electrical conductivity. $Pb_8Sb_8S_{15}Te_5$ might be only one representative of a series of novel sulfide tellurides that combine the structural diversity of sulfides with the metallic bonding character of tellurides.

In summary, it is possible to bypass the shortcomings of electron crystallography but still exploit its benefits by combining electron microscopy and synchrotron diffraction methods. Although the limited availability of synchrotron beams may restrict the described procedure to selected cases, it may become a reliable routine for the structural characterization of microcrystalline heterogeneous samples or even intergrown domains, including the products of complex phase transitions or decomposition phenomena. In addition, it opens a perspective for the study of reaction pathways and intermediates, which are often metastable and poorly crystalline. By using inert-gas equipment,[11] the characterization of air- or moisture-sensitive samples is also feasible. This new and non-classical approach to obtaining unusual solid-state compounds enables efficient chemical and structural characterization as a first step, followed by targeted synthesis instead of the usual tedious synthesis optimization by trial and error.

Experimental Section

Heterogeneous bulk samples were synthesized in silica glass ampoules under inert conditions, starting from the elements, with a nominal composition corresponding to $Pb_5Sb_4S_6Te_5$. The samples were slowly heated to 450 °C (ca. 30 K h^{-1}), held at this temperature for 12 h, then heated to 900 °C (also 30 K h^{-1}) and quenched in water after 30 h. Nearly phase-pure material of $Pb_8Sb_8S_{15}Te_5$ was obtained by quenching small fractions of stoichiometric melts in H_2O followed by annealing the finely ground material for 16 d at 450 °C. PXRD was carried out on finely ground samples fixed on Mylar foils on a flat sample holder. For TEM measurements, the ground sample was suspended in ethanol and deposited on a copper grid coated with a holey carbon film. This grid was fixed on a glass capillary for single-

crystal X-ray diffraction. Data were collected at the European Synchrotron Radiation Facility. The thermal diffusivity was determined by using the laser flash method, while the resistivity was measured in a four-point setup simultaneously with the Seebeck coefficient. Further details are given in the Supporting Information.

Keywords: electron microscopy · microcrystals · microfocus synchrotron diffraction · structure elucidation · sulfide tellurides

How to cite: *Angew. Chem. Int. Ed.* **2015**, *54*, 10020–10023
Angew. Chem. **2015**, *127*, 10158–10161

[1] a) U. Kolb, E. Mugnaioli, T. E. Gorelik, *Cryst. Res. Technol.* **2011**, *46*, 542–554; b) E. Mugnaioli, I. Andrusenko, T. Schüler, N. Loges, R. E. Dinnebier, M. Panthöfer, W. Tremel, U. Kolb, *Angew. Chem. Int. Ed.* **2012**, *51*, 7041–7045; *Angew. Chem.* **2012**, *124*, 7148–7152; c) H. Klein, *Z. Kristallogr.* **2013**, *228*, 35–42; d) T. Willhammar, X. Zou, *Z. Kristallogr.* **2013**, *228*, 11–27; e) G. van Tendeloo, S. Bals, S. van Aert, J. Verbeeck, D. van Dyck, *Adv. Mater.* **2012**, *24*, 5655–5675; f) U. Schürmann, V. Duppel, S. Buller, W. Bensch, L. Kienle, *Cryst. Res. Technol.* **2011**, *46*, 561–568; g) L. Palatinus, D. Jacob, P. Cuvillier, M. Klementova, W. Sinkler, L. D. Marks, *Acta Crystallogr. Sect. A* **2013**, *69*, 171–188; h) L. Palatinus, V. Petrícek, C. A. Corrêa, *Acta Crystallogr. Sect. A* **2015**, *71*, 235–244; i) G. B. M. Vaughan, S. Schmidt, H. F. Poulsen, *Z. Kristallogr.* **2004**, *219*, 813–825.

[2] a) Y. Moëlo, E. Makovicky, N. N. Mozgova, J. L. Jambor, N. Cook, A. Pring, W. Paar, E. H. Nickel, S. Graeser, S. Karup-Møller, T. Balic-Žunic, W. G. Mumme, F. Vurro, D. Topa, L. Bindi, K. Bente, M. Shimizu, *Eur. J. Mineral.* **2008**, *20*, 7–46; b) T. Srikrishnan, W. Nowacki, *Z. Kristallogr.* **1974**, *140*, 114–136; c) A. Pring, B. Etschmann, *Mineral. Mag.* **2002**, *66*, 451–458; d) N. N. Mozgova, Z. V. Vrubilevskaya, A. V. Sivtsov, *Dokl. Akad. Nauk SSSR* **1984**, *274*, 169–172.

[3] a) T. Rosenthal, M. N. Schneider, C. Stiewe, M. Döblinger, O. Oeckler, *Chem. Mater.* **2011**, *23*, 4349–4356; b) P. P. Konstantinov, L. E. Shelimova, E. S. Avilov, M. A. Kretova, V. S. Zemskov, *Inorg. Mater.* **2001**, *37*, 662–668; c) P. Urban, M. N. Schneider, L. Erra, S. Welzmiller, F. Fahrnbauer, O. Oeckler, *CrystEngComm* **2013**, *15*, 4823–4829.

[4] a) L. Pauling, *Am. Mineral.* **1975**, *60*, 994–997; b) H. Liu, L. L. Y. Chang, *Am. Mineral.* **1994**, *79*, 1159–1166; c) D. C. Grauer, Y. S. Hor, A. J. Williams, R. J. Cava, *Mater. Res. Bull.* **2009**, *44*, 1926–1929; d) S. V. Eremeev, Yu. M. Koroteev, E. V. Chulkov, *JETP Lett.* **2010**, *91*, 387–391.

[5] a) P. Bayliss, *Am. Mineral.* **1991**, *76*, 257–265; b) H. Liu, L. L. Y. Chang, *Mineral. Mag.* **1994**, *58*, 567–578.

[6] a) A. Skowron, I. D. Brown, *Acta Crystallogr. Sect. C* **1990**, *46*, 531–534; b) W. G. Mumme, *Neues Jahrb. Mineral. Monatsh.* **1989**, 498–512.

[7] S. Lobe, *Master thesis*, Leipzig University, **2009**.

[8] Crystal data for $Pb_8Sb_8S_{15}Te_5$: Heavy-duty diffractometer (Huber, Germany) with FReLoN2K CCD detector (dynamical range 2^{16}; J.-C. Labiche, O. Mathon, S. Pascarelli, M. A. Newton, G. G. Ferre, C. Curfs, G. Vaughan, A. Homs, D. F. Carreiras, *Rev. Sci. Instrum.* **2007**, *78*, 091301) at the European Synchrotron Radiation Facility (Materials Science Beamline ID11, Grenoble, France; G. B. M. Vaughan, J. P. Wright, A. Bytchkov, C. Curfs, C. Grundlach, M. Orlova, L. Erra, H. Gleyzolle, T. Buslaps, A. Götz, G. Suchet, S. Petitdemange, M. Rossat, L. Margulies, W. Ludwig, A. Snigirey, I. Snigireva, H. O. Sorensen, E. M. Lauridsen, U. L. Olsen, J. Oddershede, H. F. Poulsen, *Challenges in Materials Science Possibilities in 3D and 4D Characterization Techniques: Proceedings of the 31st Risø International Symposium on Materials Science* **2010**, 457–476), $\lambda = 0.29460$ Å, $M = 3750.4\ g\,mol^{-1}$, crystal size $0.3 \times 0.5 \times 1\ \mu m^3$, space group $P4_1$, $a = 8.0034(4)$ Å, $c = 15.0216(5)$ Å, $V = 962.2(1)$ Å^3, $Z = 1$, X-ray density $\rho = 6.472\ g\,cm^{-3}$, $\mu = 8.57\ mm^{-1}$, $T = 293(2)$ K, 5285/2357 meas./indep. reflections, semiempirical absorption correction (SADABS, v2.03, Bruker AXS, Madison, USA, **1999**), least-squares refinement (all atoms anisotropic; SHELX-97, G. M. Sheldrick, *Acta Crystallogr. Sect. A* **2008**, *64*, 112–122), 90 parameters, 3 restraints, $R_\sigma = 0.0651$, $R_{int} = 0.0346$, *R1* (obs./all) = 0.0373/0.0387, *wR2* (obs./all) = 0.0984/0.0994, residual electron density (min./max.) = −1.79/1.53. Further details of the crystal structure investigation may be obtained from the Fachinformationszentrum Karlsruhe, 76344 Eggenstein-Leopoldshafen, Germany (fax: (+49) 7247-808-666; e-mail: crysdata@fizkarlsruhe.de), on quoting the depository number CSD-427208.

[9] a) H.-L. Keller, *Z. Anorg. Allg. Chem.* **1977**, *432*, 141–146; b) H.-L. Keller, *J. Less-Common Met.* **1981**, *78*, 281–286.

[10] a) P. M. Skarstad, C. R. Hubbard, R. S. Roth, H. S. Parker, *J. Solid State Chem.* **1979**, *30*, 65–78; b) A. Ferrier, M. Velázquez, O. Pérez, D. Grebille, X. Portier, R. Moncorgé, *J. Cryst. Growth* **2006**, *291*, 375–384.

[11] P. Jeitschko, A. Simon, R. Ramlau, Hj. Mattausch, *Z. Anorg. Allg. Chem.* **1997**, *623*, 1447–1454.

Received: April 21, 2015
Published online: July 24, 2015

